ARTICLE

Poly(arylene ether)s Containing Superacid Groups as Proton Exchange Membranes

Takefumi Mikami,[†,‡] Kenji Miyatake,*[,†,§] and Masahiro Watanabe*[,†]

Fuel Cell Nanomaterials Center and Clean Energy Research Center, University of Yamanashi, 4 Takeda, Kofu, Yamanashi 400-8510, Japan, and Yamanashi Prefectural Industrial Technology Center, 2094 Otsumachi, Kofu, Yamanashi 400-0055, Japan

ABSTRACT A series of poly(arylene ether)s containing pendant superacid groups on fluorenyl groups were synthesized and their properties were investigated for fuel cell applications. Poly(arylene ether)s containing iodo groups were synthesized by the polymerization of 2,7-diiodo-9,9-bis(4-hydroxyphenyl)fluorene with difluorinated compounds such as decafluorobiphenyl, bis(4-fluorophenyl)sulfone, and bis(4-fluorophenyl)ketone, under nucleophilic substitution conditions. The iodo groups on the fluorenyl groups were converted to perfluorosulfonic acid groups via the Ullmann coupling reaction. The degree of perfluorosulfonation was controlled to be up to 92%, which corresponds to an ion exchange capacity (IEC) of 1.52 meq/g. The ionomers yielded flexible, ductile membranes by solution casting. The ionomer membranes exhibited a characteristic hydrophilic/hydrophobic phase separation, with small interconnected hydrophilic clusters (2−3 nm), which is similar to that of the benchmark perfluorinated membrane (Nafion). The aromatic ionomers containing superacid groups showed much higher proton conductivities than those of the conventional sulfonated aromatic ionomers with similar main chain structures. Fuel cell performance with the superacidic ionomer membranes was also tested.

KEYWORDS: poly(arylene ether)s • proton exchange membranes • ionomers • fuel cells • ion conductive polymers

INTRODUCTION

Polymer electrolyte membrane fuel cells (PEMFCs) are regarded as a source of clean energy because of features such as high efficiency, high energy density, and environmental friendliness. Polymer electrolyte membranes that transport protons from anode to cathode are one of the key materials of PEMFCs. Perfluorosulfonic acid (PFSA) polymers such as Nafion (DuPont) are most used because of their high chemical and physical stability along with high proton conductivity. PFSA polymers, however, suffer from several problems, including high production cost, environmental incompatibility, and limited operation temperature in fuel cells (1). These issues have stimulated the research to develop alternative polymer electrolyte membranes (2−5). Among these, sulfonated aromatic polymers have been investigated most extensively over the past decade. Such polymers include sulfonated poly(arylene ether)s (6, 7), poly(arylene ether sulfone)s (8−11), poly(arylene ether ether ketone)s (12−14), poly(phenylene sulfide)s (15), poly(phenylene sulfone)s (16), poly(phenylene)s (17−19), polyimides (20−22), and polybenzimidazoles (23, 24). Although aromatic polymers are generally robust under severe conditions (high temperature, strong acid, oxidizing species, water vapor, mechanical stress, etc.), sulfonic acid groups substituted onto the polymers often give rise to a deterioration of such favorable stability. Some ionomer membranes are claimed to exhibit high proton conductivity; however, the conductivities at high temperature and low humidity are lower than that of Nafion and require much improvement.

One of the reasons for the lower proton conductivity of aromatic ionomer membranes is their weaker acidity. The pK_a values of arylsulfonic acid groups are generally higher than those of perfluorosulfonic acids. For example, the pK_a value for $PhSO_3H$ is −2.5, whereas that for CF_3SO_3H is −13. The pK_a value was estimated to be ca. −1 for sulfonated polyether ketone and ca. −6 for Nafion membranes (25). Therefore, the effective proton concentration and proton mobility are lower in the aromatic ionomer membranes. Moreover, the aromatic ionomer membranes lack well-developed ionic channels because of less pronounced hydrophilic and hydrophobic phase separation. This lack also helps to account for the lower proton conductivity at low humidity.

Our recent idea for improving proton conductivity has been to introduce superacid groups onto aromatic polymers. These ionomers are regarded as an intermediate between the perfluorosulfonated and hydrocarbon ionomers and will help to understand the differences between them. In a preliminary communication (26), we reported that poly(arylene ether)s containing pendant perfluorosulfonic acid groups showed well-developed, interconnected ionic clusters, and thus high proton conductivity compared to the conventional aromatic ionomer membranes. More recently, similar results were obtained by other groups (27). In this

* Corresponding author. Tel: +81 55 220 8707 (K.M.) +81 55 254 7091 (M.W.). E-mail: miyatake@yamanashi.ac.jp (K.M.); m-watanabe@yamanashi.ac.jp (M.W.).

Received for review March 15, 2010 and accepted May 12, 2010

† Fuel Cell Nanomaterials Center, University of Yamanashi.

‡ Yamanashi Prefectural Industrial Technology Center.

§ Clean Energy Research Center, University of Yamanashi.

DOI: 10.1021/am100224z

Published on Web 05/21/2010

article, we report further investigation on the synthesis and properties of the superacid-modified poly(arylene ether)s. Synthesis of poly(arylene ether)s containing iodine-substituted fluorenyl groups and their perfluorosulfonation via the Ullmann coupling reaction were studied in detail. The effects of the superacid groups on the properties, such as thermal stability, gas permeability, proton conductivity, water affinity, and morphology, were also studied. Finally, the fuel cell performance with the superacid-modified ionomer membrane was tested.

EXPERIMENTAL SECTION

Materials. Bis(4-fluorophenyl)sulfone (FPS) and 4,4′-difluorobenzophenone (FBP) were purchased from TCI and purified by crystallization from toluene. Decafluorobiphenyl (DFB) was purchased from TCI and used as received. *N,N*-Dimethylacetamide (DMAc; organic sythesis grade, 99%) was purchased from Kanto Chemical and dried over molecular sieves (3A) prior to use. Potassium tetrafluoro-2-(tetrafluoro-2-iodoethoxy)ethanesulfonate (PFSK) was prepared by hydrolysis of tetrafluoro-2-(tetrafluoro-2-iodoethoxy)ethanesulfonyl fluoride (97%, Aldrich Chemical) according to previous reports (27, 28). Copper powders (diameter was 45 μm and 100 nm) were purchased from Aldrich Chemical. Other solvents and regents were of commercially available grade and used as received.

Monomer Synthesis. ***2,7-Diiodo-9-fluorenone (1).*** A 300-mL round-bottom flask equipped with a dropping funnel was charged with 9-fluorenone (12.5 g, 70 mmol), iodine (20.0 g, 160 mmol), carbon tetrachloride (20 mL), concentrated sulfuric acid (20 g), and glacial acetic acid (150 mL). The mixture was heated to at 80 °C, and then 30% hydrogen peroxide aqueous solution (50 mL) was added dropwise into the mixture over a period of 2 h. During the addition of hydrogen peroxide, the color of the mixture changed from dark purple to light red, and a yellow solid precipitated. The precipitate was filtered and washed with deionized water. The crude product was purified by crystallization from 2-propanol to produce yellow needle crystals of 2,7-diiodo-9-fluorenone (**1**) in 80% yield. ^{1}H NMR (400 MHz, $CDCl_3$-*d*, δ, ppm): 7.97 (s, 2H), 7.84 (d, J = 8.0 Hz, 2H), 7.28 (d, J = 8.0 Hz, 2H); MS (EI) *m/z* 432 (M^+), 305, 277, 150.

9,9-Bis(4-hydroxyphenyl)-2,7-diiodo-fluorene (2). A 300-mL round-bottom flask was charged with **1** (8.64 g, 20 mmol), phenol (11.28 g, 120 mmol), methanesulfonic acid (2.45 g, 25 mmol) and carbon tetrachloride (40 mL). The mixture was stirred at 80 °C for 40 h and poured slowly into 1 L of deionized water to precipitate a pale yellow product. The crude product was washed several times with hot deionized water and was purified by crystallization from acetone/toluene to produce white granular crystals of 9,9-bis(4-hydroxyphenyl)-2,7-diiodofluorene (**2**) in 50% yield. ^{1}H NMR (400 MHz, DMSO-d_6, δ, ppm): 9.40 (s, 2H), 7.73 (m, 4H), 7.64 (s, 2H), 6.88 (d, J = 8.4 Hz, 4H), 6.67 (d, J = 8.4 Hz, 4H); MS (EI) *m/z* 602(M^+), 475, 381, 347.

Polymer Synthesis. ***Synthesis of Polymers* 3b *and* 3c.** A typical polymerization procedure was as follows. A 100-mL round-bottom flask equipped with a Dean−Stark trap and a mechanical stirrer was charged with **2** (1.204 g, 2 mmol), FBP (0.218 g, 1 mmol), FPS (0.254 g, 1 mmol), potassium carbonate (0.691 g, 5 mmol), DMAc (6 mL), and toluene (3 mL). The mixture was stirred at 120 °C for 3 h to remove product water as a toluene azeotrope. The reaction was continued at 120 °C for 18 h under nitrogen. Then, the mixture was cooled to room temperature and poured dropwise into 200 mL of deionized water to precipitate the product. The precipitate was filtered and washed with hot water and methanol several times. Drying under vacuum at 80 °C for 16 h produced **3b** in 98% yield (1.56 g). ^{1}H NMR (400 MHz, $CDCl_3$-*d*, δ, ppm): 7.86 (d, J = 8.3 Hz, 4H), 7.77 (d, J = 8.4 Hz, 4H), 7.69−7.65 (m, 8H), 7.47 (d, J = 7.6 Hz, 4H), 7.15−7.11 (m, 8H), 7.04−7.00 (m, 8H), 6.95 (d, J = 6.2 Hz, 4H), 6.90 (d, J = 6.2 Hz, 4H). Polymer **3a** was synthesized as described previously (26).

Perfluorosulfonation. A typical perfluorosulfonation procedure was as follows. A 100-mL round-bottom flask equipped with a nitrogen inlet and a magnetic stirrer was charged with **3b** (0.798 g), copper powder (0.636 g), and DMAc (10 mL). The mixture was stirred at 120 °C for 4 h. Then, PFSK (1.38 g) solution in 10 mL of DMAc was added dropwise to the mixture, and the reaction was continued at 160 °C for 72 h. The reaction mixture was cooled to room temperature. The copper powder was removed by filtration. The filtrate was poured dropwise into 200 mL of 2 M HNO_3 to precipitate a product. The crude product was filtered, reprecipitated from DMAc/2 M HNO_3 several times, and washed with deionized water. Drying under a vacuum at 80 °C for 16 h produced a pale yellow powder of **4b**. ^{1}H NMR (400 MHz, DMSO-d_6, δ, ppm): 8.23 (d, J = 7.5 Hz, 4H), 7.83 (d, J = 8.6 Hz, 4H), 7.78 (d, J = 6.9 Hz, 4H), 7.72−7.67 (m, 8H), 7.19−7.16 (m, 8H), 7.09−6.99 (m, 16H),^{19}F NMR (376 MHz, DMSO-d_6, δ, ppm): −81.8 (2F), −86.1 (2F), −111.5 (2F), −117.1 (2F).

Membrane Preparation. A DMAc solution of **4** was filtered and cast onto a flat glass plate. Drying the solution at 50 °C under atmospheric pressure for 15 h yielded a pale yellow, ductile membrane. The membrane was immersed in 1 M HNO_3 for 24 h. The acidification process was repeated three times. The membrane was then washed with deionized water several times and dried under a vacuum at 80 °C for 16 h. The membrane in acid form was obtained with a thickness of ca. 40 μm.

Measurements. ^{1}H and ^{19}F NMR experiments were performed on a Bruker AVANCE 400S spectrometer using deuterated dimethyl sulfoxide (DMSO-d_6) or deuterated chloroform ($CDCl_3$) as the solvent and tetramethylsilane (TMS) as the internal reference, respectively. Molecular weight measurement was performed via gel permeation chromatography on an instrument equipped with two polystyrene gel columns (Shodex KF-805, 806) and a JASCO 875 UV detector set at 300 nm. *N,N*-Dimethylformamide containing 0.01 M LiBr was used as the eluent at a flow rate of 1.0 mL/min. M_w and M_n were calibrated with standard polystyrene samples.

Ion Exchange Capacity (IEC). The IEC values of the **4** membranes were determined by titration and ^{19}F-NMR spectroscopy (**4a** only). In the titration method, a section of the membrane was equilibrated in a large excess of 0.2 M NaCl aqueous solution for 40 h. The HCl released by ion-exchange was measured by titration with 0.01 N NaOH aqueous solution using an Auto Potentiometric titrator (KEM AT-510). In the ^{19}F NMR method, the IEC was calculated from the integral ratio of the peaks of the side chains to the main chains.

Thermal Analyses. Thermal analyses were performed on a Mac Science thermogravimetric differential thermal analysis (TG/DTA) 2000 instrument equipped with a Bruker MS 9600 mass spectrometer. The temperature was increased from room temperature to 400 °C at a heating rate of 10 °C/min under argon.

STEM Observation. The membranes were stained with lead ions by ion exchange of the sulfonic acid groups. The membranes were immersed overnight in 1 M $Pb(CH_3COO)_2$ aqueous solution, rinsed with water and dried in a vacuum for 16 h. The stained membranes were embedded in epoxy resin and sectioned to give a 90-nm thick membrane. The images were taken on a Hitachi HD-2300C scanning transmission electron microscope (STEM) with an accelerating voltage of 200 kV.

Water Uptake and Proton Conductivity. Water uptake and proton conductivity of the membranes were measured with a solid electrolyte analyzer system MSBAD-V-FC (Bel Japan Inc.) equipped with a temperature and humidity controllable cham-

Scheme 1. Synthesis of Monomer 2

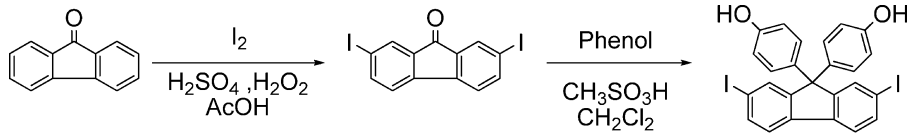

1 2

ber. For the water uptake measurement, the membranes were dried for 3 h at 80 °C under vacuum and exposed to a given humidity at least for 3 h. The weights of the membranes were measured with a magnetic suspension balance, and the water uptake (WU) was calculated from $WU = (W_{wet} - W_{dry})/W_{dry} \times 100$, where W_{wet} and W_{dry} are the weights of the hydrated and dried membranes, respectively. The in-plane proton conductivity of the membranes was measured via electrochemical impedance spectroscopy over the frequency range from 1 to 1×10^5 Hz using an impedance spectrometer (Solartron 1255B and 1287, Solartron Inc.). Membrane samples were mounted in a 4-probe conductivity cell and placed in the chamber. Proton conductivity (σ) was calculated from $\sigma = d/(AR)$, where d and A are the thickness and the conducting area, and R is the ionic resistance.

Gas Permeability. Hydrogen and oxygen gas permeabilities through the membrane were measured with a gas permeation measurement apparatus (GTR-Tech 20XFYC). The concentration of the permeated gas was quantified with a gas chromatograph (Yanaco G2700T) using a thermal conductivity detector. Argon and helium were used as a carrier gas for the measurements of hydrogen and oxygen, respectively. The permeation cell was placed in an oven, and the cell temperature was controlled. The membrane was placed in the cell, and the dry test gas (hydrogen or oxygen) was introduced onto one side of the membrane at a flow rate of 20 mL/min. Carrier gas was introduced onto the other side of membrane at a flow rate of 30 mL/min and measured with GC. The membrane was equilibrated at least 3 h before each measurement, and five separate measurements were averaged in each experiment. The gas permeability coefficient Q (cm^3 (STD) cm cm^{-2} s^{-1} cm Hg^{-1}) was calculated according to the following equation

$$Q = \frac{273}{T}\frac{1}{A}B\frac{1}{t}l\frac{1}{76}$$

where T (K) is the absolute temperature of the cell, A (cm^2) is the permeation area, B (cm^3) is the volume of the test gas permeated through the membrane, t (s) is the sampling time, and l (cm) is the thickness of the membrane.

Fuel Cell Performance. A membrane-electrode assembly (MEA) was fabricated by sandwiching a **4a** membrane with gas diffusion electrodes containing Nafion binder. The loading amount of Pt catalyst on the electrodes was 0.5 mg/cm^2. The MEA obtained was evaluated in a single cell (active area, 3.8 cm^2) with oxygen as the oxidant and hydrogen as the fuel at cell temperature of 80 °C. The fuel cell was operated at various gas humidities: 100, 78, 53, and 30% RH for both electrodes.

RESULTS AND DISCUSSION

Synthesis of Monomer and Polymers. A new monomer having iodo groups, 2,7-diiodo-9,9-bis(4-hyroxyphenyl)fluorene **2**, was synthesized referring to the brominated equivalent (29), as shown in Scheme 1. Briefly, fluorenone was reacted with iodine in a mixture of acetic acid, hydrogen peroxide, and sulfuric acid to obtain 2,7-diiodofluoreneone **1**, which was reacted with phenol in carbon tetrachloride in the presence of methanesulfonic acid to produce **2**. The yield of **2** was 50%, which was lower than for the unsubstituted fluorenone (95%), probably because of the steric hindrance of the iodo groups.

Monomer **2** was polymerized with difluorinated compounds under typical nucleophilic substitution polymerization conditions to yield polymers **3a**–**c**, where **3a** contained perfluorobiphenyl groups in the main chain, **b** was a 1:1 copolymer of diphenyl sulfone and benzophenone, and **c** contained benzophenone groups (Scheme 2). The polymerization results are summarized in Table 1. The polymerization was conducted at low temperature (<120 °C) in order to avoid the reaction and elimination of the iodo groups. Due to the high reactivity of decafluorobiphenyl, the highest molecular weight (M_w = 740 kDa) was achieved with **3a**. The molecular weight distribution of **3a** was broad for a polycondensation reaction. The results may suggest that a minor amount of branched and/or cross-linked structure was involved, along with the preferred reaction of decafluorobiphenyl at the 4,4′-positions.

Attempts to obtain even higher molecular weights for **3a** by elevating the polymerization temperature were not successful and produced an insoluble product. Polymerization of **2** with FPB or FPS was not very successful and produced low-molecular-weight **3c** (M_w = 32 kDa) or insoluble **3d** polymers. Therefore, copolymer **3b** containing FPS and FPB (50/50) was synthesized. Compared to each of the corresponding homopolymers, copolymer **3b** was higher in molecular weight (M_w = 67 kDa), with better solubility in DMAc. The chemical structure of the polymers **3a**–**c** was analyzed by ^{1}H and ^{19}F NMR spectra. For example, two sets of doublet peaks at 6.94 and 7.14 ppm were assigned to 1,4-phenylene protons, and another two sets of doublet peaks at 7.48 and 7.69 ppm and a singlet peak at 7.65 ppm were assigned to iodine-substituted fluorenyl protons in the ^{1}H NMR spectrum of **3a** (see the Supporting Information). In the ^{19}F NMR spectrum, two singlet peaks were observed and assigned to octafluoro-4,4′-biphenylene fluorine groups. These NMR data support the formation of the supposed structure of the polymers.

Perfluorosulfonation of Polymers. To introduce perfluorosulfonic acid groups, polymers **3a**–**c** were reacted with potassium tetrafluoro-2-(tetrafluoro-2-iodoethoxy)ethanesulfonate (PFSK) in the presence of Cu powder via the Ullmann reaction. The Ullmann reaction was conducted in two steps: in the first step, copper powder was reacted with the polymers **3**, and in the second step, PFSK was added into the reaction mixture. After the reaction, the product was

Scheme 2. Synthesis of Polymers

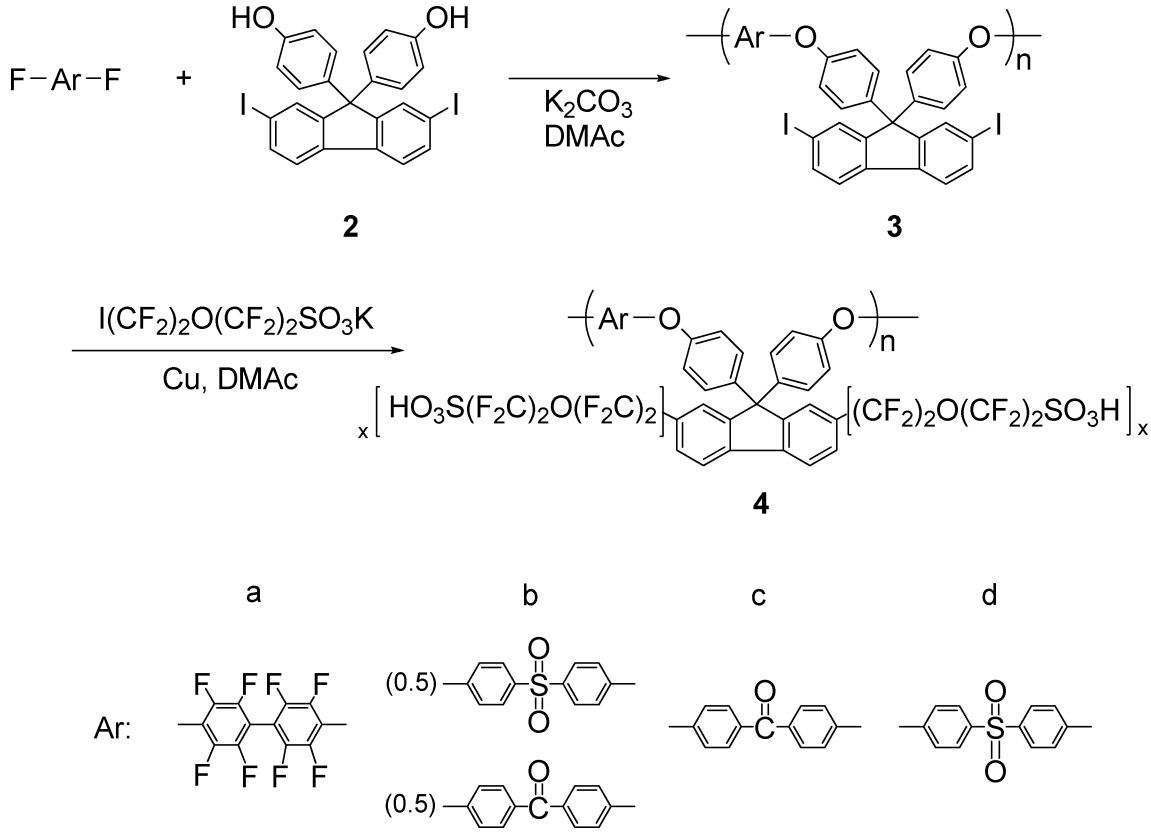

Table 1. Synthesis of Polymers 3a−d

Ar	T (°C)	reaction time (h)	M_n (kDa)	M_w (kDa)
a	60	48	9	34
a	60	96	19	105
a	90	18	31	280
a	90	24	24	465
a	100	24	30	740
a	120	24	[a]	[a]
b	100	24	12	37
b	120	24	26	47
b	120	18	21	67
c	120	24	4	15
c	120	24	5	32
d	120	18	[a]	[a]

[a] Insoluble.

Table 2. Synthesis of Polymers 4a−c

	first step			second step			
Ar	T (°C)	time (h)	diameter of Cu (μm)	T (°C)	time (h)	degree of perfluoro-sulfonation (%)	IEC (meq/g)
a[a]	120	4	45	160	72	25	0.51
a[b]	120	4	0.1	160	40	46	0.87
a[c]	120	4	0.1	160	40	54	1.00
a[a]	120	4	0.1	160	40	82	1.40
a[d]	120	4	0.1	120	36	92	1.52
b	120	2	0.1	160	72	68	1.32
b	120	4	0.1	160	72	76	1.44
c	100	4	0.1	160	40	60	1.21

[a] M_w = 280 kDa (as **3a**). [b] M_w = 740 kDa (as **3a**). [c] M_w = 465 kDa (as **3a**). [d] M_w = 105 kDa (as **3a**).

recovered by removing the excess copper and PFSK. The perfluorosulfonated polymers **4** were obtained as flakes. They were soluble in polar aprotic solvents such as DMSO, DMAc, DMF, and NMP, and partly soluble in acetone, methanol, and ethanol. Casting from the solutions produced pale brown, transparent films of **4**. Among these, **4a** produced tough, ductile membranes because of its high molecular weight. The degree of perfluorosulfonation was estimated from the titration.

The results of the perfluorosulfonation reaction are summarized in Table 2. The particle size of copper was crucial for this reaction: the degree of perfluorosulfonation (x in Scheme 2) in **4a** was >46% with small particles of Cu (100 nm) and was much lower (25%) when large particles of Cu (45 μm) were used. Optimization of the reaction conditions led to the achievement of 92% perfluorosulfonation for **4a**. Unlike typical Ullmann reactions, higher temperatures and longer times (in the second step) did not necessarily promote higher conversion, probably because of the possible elimination of the iodo groups. Otherwise, it turned out that the molecular weight of the polymers was the more important factor. As shown in rows 2−5 in Table 2, polymer **3a** samples of different molecular weights (M_w = 105−740 kDa) were reacted under the same conditions. The reaction mixture was heterogeneous because of the presence of the Cu powder, and the higher-molecular-weight polymers engendered increased viscosity of the mixture, thus decreasing the efficiency of the reaction. Therefore, the higher molec-

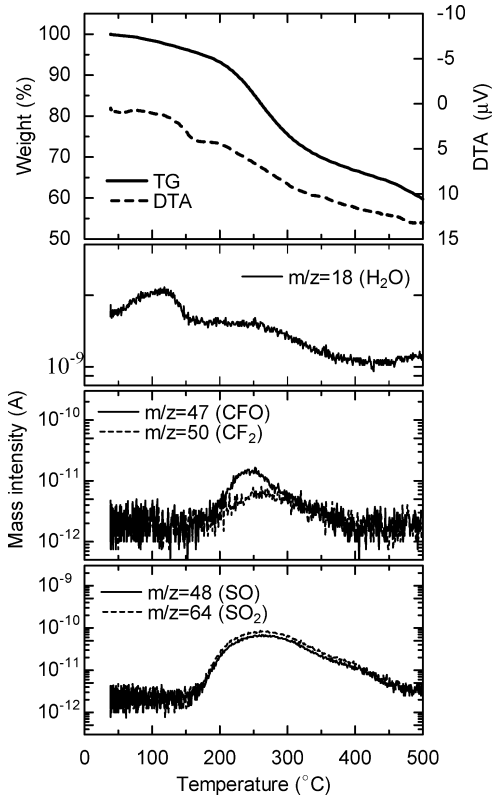

FIGURE 1. TG/DTA and MS curves of 4a (IEC = 1.52 meq/g) under a dry argon atmosphere.

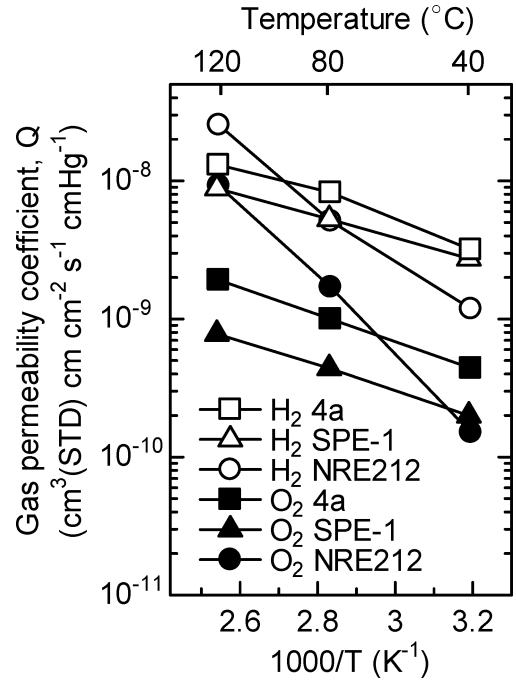

FIGURE 2. Temperature dependence of hydrogen and oxygen permeability of 4a (IEC = 0.87 meq/g), SPE-1 (IEC = 1.63 meq/g), and Nafion NRE212 (IEC = 0.91 meq/g) membranes under dry conditions (the error was within 8%).

ular weight polymers yielded lower degrees of perfluorosulfonation. The highest degree of perfluorosulfonation (92%) was achieved with the polymer with M_w = 105 kDa to produce polymer **4a** with IEC = 1.52 meq/g. Polymers **4b** and **4c** were also obtained in the same manner from **3b** and **3c**, respectively. The IEC values of the **4b** and **4c** membranes ranged from 1.21 to 1.44 meq/g, comparable to those of the **4a** membranes.

The chemical structure of the polymers **4a**−**c** was analyzed by ^{1}H and ^{19}F NMR spectra. In the ^{1}H NMR spectrum of **4a** (IEC = 1.52 meq/g) (26), the peaks were well-assigned to the oxyphenylene main chains and 2,7-disubstituted fluorenylidene groups. The six peaks in the ^{19}F NMR spectrum, ranging from −81.9 to −153.6 ppm, were assignable to the fluorine groups in the main and the side chains. The integral ratio in the ^{19}F NMR spectrum enabled us to calculate an IEC of 1.62 meq/g, which is in fair agreement with the IEC obtained by titration. The ^{1}H and ^{19}F NMR spectra of **4b** (IEC = 1.44 meq/g) and their assignment are provided in the Supporting Information. The densities of these ionomers were ca. 1.6 g/cm^3, and slightly higher than those of the conventional sulfonated aromatic ionomers.

Thermal Stability. The thermal stability of **4a** (IEC = 1.52 meq/g) was investigated by TG/DTA-MS analysis (Figure 1). A dry membrane sample in the acid form was subjected to the measurement under argon atmosphere. In the TG curve, the first weight loss observed after heating from room temperature was due to the evaporation of hydrated water, as confirmed by the mass chromatogram of water (m/z = 18). The second weight loss from ca. 180 to 300 °C was assigned to the decomposition of the pendant perfluorosulfonic acid groups. In the mass chromatograms, major fragment ions observed in the second weight loss were SO (m/z = 48), SO_2 (m/z = 64), CFO (m/z = 47), and CF_2 (m/z = 50). The thermal degradation behavior of **4a** was similar to that of our previous poly(arylene ether) ionomers with sulfonic acid groups directly attached to the fluorenylidene groups (10). Loss of perfluorosulfonic acid groups occurred at lower temperature for **4a** than for Nafion (ca. 280 °C), indicating that aromatic perfluorosulfonic acid groups are less thermally stable than those on Teflon-like poly(tetrafluoroethylene) main chains. In the DTA curve of **4a**, a glass transition was not observed up to the decomposition temperature.

Gas Permeability. Hydrogen and oxygen permeabilities of the perfluorosulfonated polymer **4a** membrane (IEC = 0.87meq/g) were measured under dry conditions and plotted as a function of temperature (40, 80, and 120 °C) in Figure 2. For comparison, data for SPE-1 (our previous sulfonated poly (arylene ether sulfone) without superacid groups) (10) and Nafion NRE212 membranes are also included. The hydrogen and oxygen permeabilities of the **4a** membrane were higher than those of the Nafion membrane at 40 °C and lower at 120 °C. The ratios of hydrogen and oxygen permeabilities of **4a** to those of Nafion were ca. 1/2 and 1/5 at 120 °C, respectively. The difference between hydrogen and oxygen probably comes from the fact that the perfluorinated Nafion membrane has a higher affinity for oxygen than **4a**. Membrane **4a** showed higher hydrogen and oxygen permeabilities than those of the SPE-1 membrane at all temperatures examined. The higher gas permeability of **4a** was more apparent for oxygen than hydrogen, because of the partial fluorinated structure of **4a** both in the main

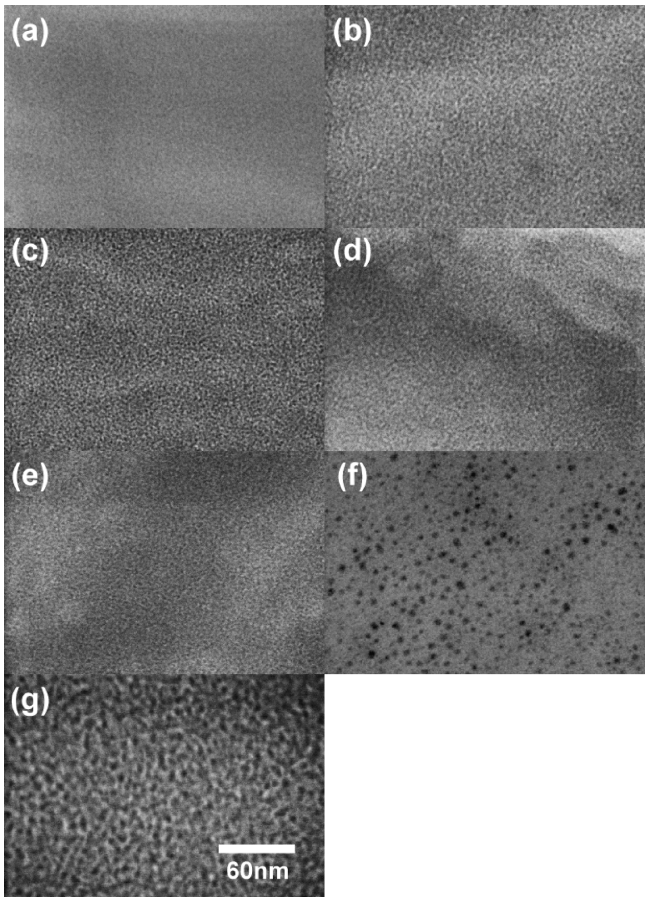

FIGURE 3. STEM images of (a) 4a (0.87 meq/g), (b) 4a (1.40 meq/g), (c) 4a (1.52 meq/g), (d) 4b (1.32 meq/g), (e) 4c (1.21 meq/g), (f) SPE-1 (1.59 meq/g), (g) Nafion NRE212 (0.91 meq/g).

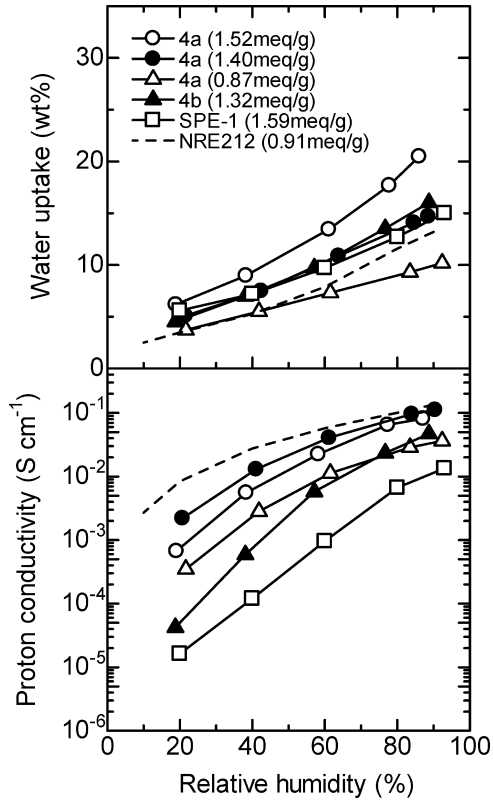

FIGURE 4. Humidity dependence of the water uptake and proton conductivity of 4a (IEC = 0.87, 1.40, and 1.52 meq/g), 4b (IEC = 1.32 meq/g), SPE-1 (IEC = 1.59 meq/g), and Nafion NRE212 (IEC = 0.91 meq/g) membranes at 80 °C (two different samples were measured and the error was within ca. 5%).

and the side chains. The gas permeation showed approximate Arrhenius-type temperature dependence, and the activation energy for gas permeation was estimated from the slope. The apparent activation energies of the gas permeability were $E_a(H_2) = 16$ and $E_a(O_2) = 19$ kJ/mol (**4a**), $E_a(H_2) = 15$ and $E_a(O_2) = 17$ kJ/mol (SPE-1), and $E_a(H_2) = 39$ and $E_a(O_2) = 53$ kJ/mol (Nafion NRE212). The $E_a(H_2)$ and $E_a(O_2)$ of **4a** were lower than those of Nafion, and similar to those of SPE-1, because **4a** and SPE-1 have a similar rigid structure of aromatic main chains.

Morphology. The morphology of **4** membranes was investigated by STEM observation. The STEM images of **4a** (IEC = 0.87, 1.40, 1.52 meq/g), **4b** (1.32 meq/g) and **4c** (1.21 meq/g) are compared with those of SPE-1 (1.59 meq/g) and Nafion NRE212 (0.91 meq/g) membranes in Figure 3. Because the samples were stained with lead ions by ion exchange, dark and light areas correspond to hydrophilic and hydrophobic domains, respectively. In the image of the **4a** membrane of low IEC (0.87 meq/g), hydrophilic/hydrophobic phase separation was rather obscure. The phase separation was more distinct with the higher IEC membranes. The **4a** membranes with IEC = 1.40 and 1.52 meq/g exhibited small hydrophilic clusters of ca. 2−3 nm in diameter distributed throughout the field of view. The **4a**, **4b**, and **4c** membranes revealed similar morphology, indicating that the main chain structure had a minor effect on membrane morphology. The morphology of the **4** membranes was distinct from that of the SPE-1 membrane. In the former membranes, the hydrophilic clusters were interconnected, whereas the clusters were larger but separated from one another in the latter membrane. The morphology of the **4** membranes was more similar to that of the Nafion membrane, in which the hydrophilic clusters were ca. 5−6 nm in diameter. It is considered that the pendant perfluorosulfonic acid groups are more likely to aggregate and form larger clusters than the arylsulfonic acid groups because of their higher polarity and flexibility. Rigid aromatic main chains compared to fluorinated aliphatic main chains of Nafion would be responsible for the smaller hydrophilic clusters.

Water Uptake and Proton Conductivity. The humidity dependences of the water uptake and proton conductivity of **4a** and **4b** membranes in the acid form were measured at 80 °C (Figure 4). In the same series of membranes (**4a**), higher IEC membranes absorbed more water, as expected. Membrane **4a** (IEC = 1.40 meq/g) showed slightly lower water uptake than that of **4b** (IEC = 1.32 meq/g) despite the former's higher IEC. The results seem reasonable, taking into account the fact that **4a** contains more hydrophobic perfluorobiphenylene moieties than that of **4b** with diphenyl sulfone and diphenyl ketone units. Comparison between **4** and SPE-1 membranes revealed that the superacid-modified SPE membranes absorbed more water. For better comparison among the different IEC membranes,

the number of absorbed water molecules per sulfonic acid group (often designated as λ) was calculated to be 5.7 (**4a**, 0.87 meq/g), 5.3 (**4a**, 1.40 meq/g), 6.7 (**4a**, 1.52 meq/g), 6.0 (**4b**, 1.32 meq/g), 4.5 (SPE-1, 1.59 meq/g), and 7.1 (Nafion, 0.91 meq/g) at 80% RH. The λ values of the **4a** and **4b** membranes were higher than that of SPE-1. The λ value of the **4a** membrane with the highest IEC (1.52 meq/g) was close to that of Nafion. The larger λ of **4a** and **4b** compared to that of SPE-1 prompted us to conceive the idea that the superacid groups are more hydrophilic than the aromatic sulfonic acid groups. It was rather surprising that the **4a** membrane (IEC =1.52 meq/g) exhibited substantially higher water uptake than **4a** (IEC = 1.40 meq/g). As discussed above, **4a** (IEC =1.52 meq/g) was lower in molecular weight (M_w = 105 kDa as **3a**) and **4a** (IEC =1.40 meq/g) was higher in molecular weight (M_w = 280 kDa as **3a**). A possible explanation for the large water uptake of **4a** (IEC = 1.52 meq/g) would be that the membrane of low molecular weight has lower dimensional stability (i.e., it has a greater tendency to swell).

The superacid-modified **4a**–**c** membranes showed considerably higher proton conductivity than that of SPE-1 over the humidity range from 20 to 90% RH. Furthermore, **4a** showed a smaller dependence of proton conductivity on humidity than SPE-1. The proton conductivity of **4a** (IEC = 1.52 meq/g) was 41 times higher than that of SPE-1 (1.59 meq/g) at 20% RH, whereas they shared similar IEC values. The results clearly demonstrate that the superacid groups significantly improve the proton conductivity of the SPE membranes, because the superacid groups can utilize water molecules more efficiently for proton conduction. The **4a** (IEC = 1.40 meq/g) membrane showed higher proton conductivity than **4a** (IEC = 1.52 meq/g) despite the former's lower IEC and lower water uptake. We do not have a reasonable explanation for this behavior. The major difference between the two membranes is the molecular weight, which might affect the connectivity of the ionic channels and thus the proton mobility.

The proton conductivities of the **4a** and **4b** membranes are plotted as a function of λ and compared with those of the SPE-1 and Nafion membranes in Figure 5. The **4a** (IEC = 1.40 meq/g) membrane showed the best behavior, nearly comparable to that of the Nafion membrane. At λ = 2, the proton conductivity of **4a** (IEC = 1.40 meq/g) membrane was 135 times higher than that of SPE-1 (IEC = 1.59 meq/g). In other words, the **4a** membrane required merely half the number of water molecules required by the SPE-1 membrane to achieve the same conductivity. The results further prove that the superacid groups are effective in improving the proton-conducting properties of the SPE membranes without increasing the IEC values.

Fuel Cell Performance. Figure 6 shows the cell voltages and ohmic resistances of a fuel cell with a **4a** (IEC = 1.40 meq/g, thickness = 40 μm) membrane at 80 °C under various humidity conditions. The open circuit voltage (OCV) was 1.06 V at 30% RH, 1.05 V at 53% RH, 1.04 V at 78% RH, and 1.02 V at 100% RH, suggesting that gas

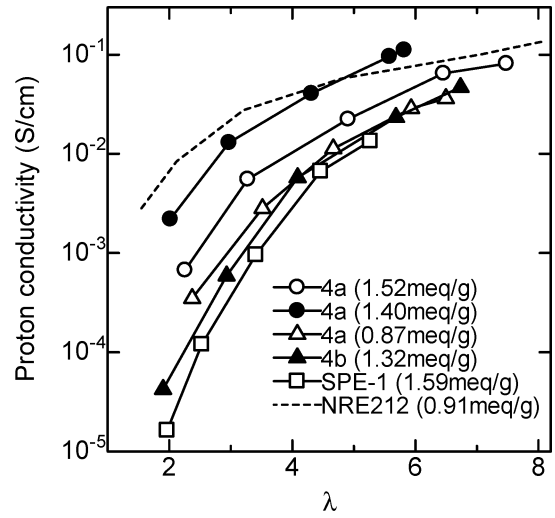

FIGURE 5. Proton conductivity of 4a (IEC = 1.52, 1.40, and 0.87 meq/g), 4b (IEC = 1.32 meq/g), SPE-1 (IEC = 1.59 meq/g), and Nafion NRE212 (IEC = 0.91 meq/g) membranes at 80 °C as a function of λ.

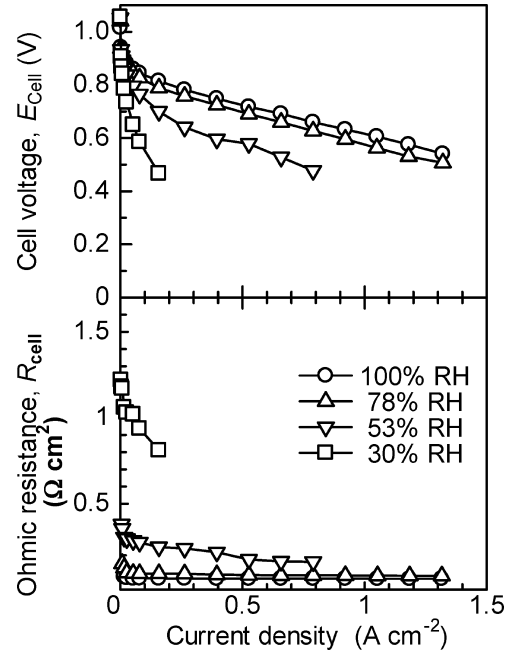

FIGURE 6. Cell voltage and ohmic resistance of H_2/O_2 fuel cells with 4a (IEC = 1.40 meq/g) membrane at 80 °C and 30, 53, 78, or 100% RH.

crossover through the membrane was negligible. The minor decrease in OCV with increasing humidity is due to the lowered oxygen partial pressure. Good fuel cell performance was obtained at high humidity (78 and 100% RH); however, the performance became worse with decreasing humidity. At 30% RH, the highest current obtainable was only 200 mA/cm^2. The decreased performance was mainly due to the increased ohmic resistance. Under low humidity conditions, the ohmic resistance was high at low current densities but decreased with increasing current density, since the water produced at the cathode helped to humidify the membrane.

The ohmic resistance was calculated from the proton conductivity data in Figure 4 to be 0.80 Ω cm^2 (30% RH), 0.14 Ω cm^2 (53% RH), 0.056 Ω cm^2 (78% RH), and 0.033

Table 3. Ohmic Resistances Observed in the Fuel Cell

method	current density (mA/cm^2)	Ohmic resistance (Ω cm^2) 30% RH	53% RH	78% RH	100% RH
measd	16	1.06	0.30	0.17	0.076
	160	0.81	0.25	0.094	0.065
	1050			0.081	0.064
calcd[a]		0.80	0.14	0.056	0.033

[a] Calculated from the proton conductivity data in Figure 4.

$\Omega \cdot$ cm^2 (100% RH) (Table 3). The experimentally obtained values of the ohmic resistance were somewhat higher than the calculated values, even under high current density conditions. The differences probably come from low gas utilization (hydrogen utilization was 2% at 160 mA/cm^2 or 13% at 1050 mA/cm^2, and oxygen utilization was 1% at 160 mA/cm^2 or 6.5% at 1050 mA/cm^2) of this fuel cell, which could dry the membrane even at high humidity. There might be some minor contact resistance (on the order of several tens of mΩ cm^2) at 100% RH between the **4a** membrane and the Nafion-based gas diffusion electrodes because of the different nature of these ionomer materials.

CONCLUSION

A new class of aromatic polymer electrolytes containing pendant superacid groups was synthesized for fuel cell applications. The precursor polymers containing iodo groups on fluorenyl groups were obtained with high molecular weights under nucleophilic substitution polymerization conditions. The perfluoroalkylsulfonic acid groups were introduced via the Ullmann reaction, in which the diameter of the Cu particles and the molecular weight of the precursor polymers were crucial. The superacid-modified ionomers showed thermal and gas permeation properties similar to those of the conventional sulfonated aromatic ionomers (SPE-1). In contrast, the morphology of the superacid-modified ionomer membranes was more similar to that of Nafion. Well-developed hydrophilic/hydrophobic phase separation was observed, while the hydrophilic clusters were smaller than those of Nafion. The superacid-modified ionomer membranes showed much higher proton conductivity than that of the SPE-1 membranes with similar IEC values over a wide range of humidity. A fuel cell was operated with the superacid-modified membrane at 80 °C; however, the proton conductivity must be further improved in order to function better at low humidity.

Acknowledgment. This work was partly supported by the New Energy and Industrial Technology Development Organization (NEDO) through the Research on Nanotechnology for High-Performance Fuel Cells (HiPer-FC) Project, and the Ministry of Education, Culture, Sports, Science and Technology (MEXT) Japan through a Grant-in-Aid for Scientific Research (20350086).

Supporting Information Available: ^{1}H and ^{19}F NMR spectra of monomer and polymers (PDF). This material is available free of charge via the Internet at http://pubs.acs.org.

REFERENCES AND NOTES

(1) Mauritz, K. A.; Moore, R. B. *Chem. Rev.* **2004**, *104*, 4535–4586.
(2) Hickner, M. A.; Ghassemi, H.; Kim, Y. S.; Einsla, B. R.; McGrath, J. E. *Chem. Rev.* **2004**, *104*, 4587–4611.
(3) Hickner, M. A.; Pivovar, B. S. *Fuel Cells* **2005**, *5*, 213–229.
(4) Rikukawa, M.; Sanui, K. *Prog. Polym. Sci.* **2000**, *25*, 1463–1502.
(5) Higashihara, T.; Matsumoto, K.; Ueda, M. *Polymer* **2009**, *50*, 5341–5357.
(6) Miyatake, K.; Chikashige, Y.; Watanabe, M. *Macromolecules* **2003**, *36*, 9691–9693.
(7) Wang, L.; Meng, Y. Z.; Wang, S. J.; Shang, X. Y.; Li, L.; Hay, A. S. *Macromolecules* **2004**, *37*, 3151–3158.
(8) Wang, F.; Hickner, M.; Ji, Q.; Harrison, W.; Mecham, J.; Zawodzinski, T. A.; McGrath, J. E. *Macromol. Symp.* **2001**, *175*, 387–396.
(9) Wang, F.; Hickner, M.; Kim, Y. S.; Zawodzinski, T. A.; McGrath, J. E. *J. Membr. Sci.* **2002**, *197*, 231–242.
(10) Chikashige, Y.; Chikyu, Y.; Miyatake, K.; Watanabe, M. *Macromolecules* **2005**, *38*, 7121–7126.
(11) Miyatake, K.; Chikashige, Y.; Higuchi, E.; Watanabe, M. *J. Am. Chem. Soc.* **2007**, *129*, 3879–3887.
(12) Gil, M.; Ji, X.; Li, X.; Na, H.; Eric Hampsey, J.; Lu, Y. *J. Membr. Sci.* **2004**, *234*, 75–81.
(13) Shang, X.; Tian, S.; Kong, L.; Meng, Y. *J. Membr. Sci.* **2005**, *266*, 94–101.
(14) Liu, B.; Robertson, G. P.; Kim, D.-S.; Guiver, M. D.; Hu, W.; Jiang, Z. *Macromolecules* **2007**, *40*, 1934–1944.
(15) Miyatake, K.; Shouji, E.; Yamamoto, K.; Tsuchida, E. *Macromolecules* **1997**, *30*, 2941–2946.
(16) Schuster, M.; Kreuer, K.-D.; Andersen, H. T.; Maier, J. *Macromolecules* **2007**, *40*, 598–607.
(17) Ghassemi, H.; McGrath, J. E. *Polymer* **2004**, *45*, 5847–5854.
(18) Kobayashi, T.; Rikukawa, M.; Sanui, K.; Ogata, N. *Solid State Ionics* **1998**, *106*, 219–225.
(19) Goto, K.; Rozhanskii, I.; Yamakawa, Y.; Otsuki, T.; Naito, Y. *Polym. J.* **2009**, *41*, 95–104.
(20) Yin, Y.; Fang, J. H.; Watari, T.; Tanaka, K.; Kita, H.; Okamoto, K. *J. Mater. Chem.* **2004**, *14*, 1062–1070.
(21) Chen, S.; Yin, Y.; Kita, H.; Okamoto, K.-I. *J. Polym. Sci., Part A: Polym. Chem.* **2007**, *45*, 2797–2811.
(22) Asano, N.; Aoki, M.; Suzuki, S.; Miyatake, K.; Uchida, H.; Watanabe, M. *J. Am. Chem. Soc.* **2006**, *128*, 1762–1769.
(23) Asensio, J. A.; Borrós, S.; Gómez-Romero, P. *J. Polym. Sci., Part A: Polym. Chem.* **2002**, *40*, 3703–3710.
(24) Jouanneau, J.; Mercier, R.; Gonon, L.; Gebel, G. *Macromolecules* **2007**, *40*, 983–990.
(25) Kreuer, K. D. *J. Membr. Sci.* **2001**, *185*, 29–39.
(26) Miyatake, K.; Shimura, T.; Mikami, T.; Watanabe, M. *Chem. Commun.* **2009**, 6403–6405.
(27) Yoshimura, K.; Iwasaki, K. *Macromolecules* **2009**, *42*, 9302–9306.
(28) Yoshimura, K. JP Patent 314452, 2005.
(29) Pu, K.-Y.; Zhang, B.; Ma, Z.; Wang, P.; Qi, X.-Y.; Chen, R.-F.; Wang, L.-H.; Fan, Q.-L.; Huang, W. *Polymer* **2006**, *47*, 1970–1978.

AM100224Z